Degeneration of structural brain networks is associated with cognitive decline after ischaemic stroke

Michele Veldsman
University of Oxford https://orcid.org/0000-0003-2192-378X
Hsiao-ju Cheng
National University of Singapore
Fang Ji
National University of Singapore
Emilio Werden
Florey Institute of Neuroscience and Mental Health
Mohamed Khlif
Florey Institute of Neuroscience and Mental Health
Kwun Kei Ng
National University of Singapore
Joseph Lim
Duke-NUS Medical School
Xing Qian
National University of Singapore
Haoyong Yu
National University of Singapore
Juan Helen Zhou (helen.zhou@nus.edu.sg)
National University of Singapore https://orcid.org/0000-0002-0180-8648
Amy Brodtmann
Florey Institute of Neuroscience and Mental Health

Article

Keywords: Stroke, structural networks, cognition, neurodegeneration

Posted Date: July 9th, 2020

DOI: https://doi.org/10.21203/rs.3.rs-36274/v1

Version of Record: A version of this preprint was published at Brain Communications on September 26th, 2020. See the published version at https://doi.org/10.1093/braincomms/fcaa155.

Abstract

One third of ischemic stroke patients develop cognitive impairment. It is not known whether topographical secondary neurodegeneration within distributed brain structural covariance networks (SCNs) underlies this cognitive decline. We examined longitudinal changes in SCNs and their relationship to domain-specific cognitive decline in 73 ischemic stroke patients. Patients were scanned with magnetic resonance imaging (MRI) and assessed on five cognitive domains at subacute (3-months) and chronic (1-year) timepoints. Individual-level SCN scores of major cognitive networks were derived from MRI data at each timepoint. We found that distributed degeneration in higher-order cognitive networks was associated with cognitive impairment in subacute stroke. Importantly, faster degradation in these major cognitive SCNs over time was associated with greater decline in attention, memory, and language domains. Our findings suggest that subacute ischemic stroke is associated with degeneration of higher-order structural brain networks and degradation of these networks contribute to individual trajectories of longitudinal domain-specific cognitive dysfunction.

Introduction

Cognitive decline is common after ischaemic stroke 1,2 and is associated with poor quality of life for stroke patients 3. Cognitive decline after stroke may be global in nature, or may be associated with one or more cognitive domains, such as memory, attention or language. Surprisingly, infarct location does not closely predict the severity of the post-stroke cognitive deficit 4. Infarcts in different regions of the brain can result in similar cognitive deficits, while infarcts in the same region can result in different profiles of cognitive impairments 4. Since no single brain region works in isolation, it stands to reason that an infarct will have distributed consequences, affecting incoming and outgoing connections to the damaged area 5,6. This disruption appears to be both in terms of brain function 7 and white matter connectivity 8, which have been studied extensively in stroke 5. The impact of stroke on structural covariance networks (SCNs) has not been thoroughly investigated, despite evidence of atrophy after stroke that is remote from the infarct location 9–11. SCNs are constructed based on shared inter-regional morphological characteristics, such as grey matter volume or cortical thickness that are estimated across populations 12. These SCNs closely mirror intrinsic functional networks and have aided understanding of a diverse range of neurological diseases, including epilepsy, schizophrenia and Alzheimer's Disease 12.

Brain atrophy is a normal part of healthy aging, but is accelerated in the presence of dementia causing pathologies 13 and cerebrovascular burden 14. Across dementia subtypes, the pattern of brain atrophy mirrors the healthy structural and functional networks responsible for the dominantly impaired function 15–18. For example, language networks show widespread atrophy in patients with primary progressive aphasia where language is the dominant deficit. The integrity of the networks underlying different cognitive functions may be critical for the preserved functioning of cognitive domains after stroke.

We examined structural covariance in our discovery dataset in canonical higher-order cognitive brain networks in 73 stroke patients 3-months and 1-year after ischaemic stroke. We predicted that the integrity

of SCNs at 3-months post-stroke would reflect cognitive performance. If longitudinal changes in SCNs were to be associated with longitudinal cognitive decline, the relationship at the subacute phase is unlikely to be epiphenomenal. Therefore, to further test our hypothesis, we investigated whether changes in structural covariance networks from 3-months to 1-year post-stroke would be associated with changes in cognitive function. We tested our models in our validation dataset, an independent dataset with matched imaging and neuropsychological and cognitive testing, and performed split-half analysis for longitudinal validation.

Methods

Participants

Stroke patient data from the Cognition and Neocortical Volume after Stroke study 19 were used in this study. Our discovery dataset included data from 80 stroke patients who underwent 3 Tesla magnetic resonance imaging (MRI) and detailed neuropsychological tests at the 3-month and 1-year timepoints. Here, we refer to the 3-month timepoint as subacute and the 12-month timepoint as chronic. Three months is the most commonly used timepoint for assessing outcomes after stroke. Among eighty participants, three participants were excluded due to excessive head movement during brain scans and four participants were excluded based on the lack of image homogeneity evaluated by mean correlation after voxel-based morphometry (VBM). The remaining 73 participants (mean age 67.41 years, SD 12.13, Table 1) were included in the analysis. Our validation dataset was made up of data from 26 patients from the same cohort scanned at a later date with the same scanner, MRI sequences, and neuropsychological and cognitive testing. Matched quality control to our discovery dataset excluded three patients on the basis of excessive movement in their subacute scans. One patient lacked all cognitive data and was excluded on this basis this left a total of 22 patients (mean age 68.77 years, SD 9.65, Supplementary Materials Section 6, Table S3)). All participants gave written informed consent for the study that was approved by local hospital ethics committees in line with the Declaration of Helsinki.

Neuropsychological testing

Neuropsychological and cognitive tests were administered at each timepoint, as outlined in the published protocol 19 and detailed in Supplementary Materials Section 1, Table S1 (including percentage of missing data for each test at each timepoint; <5% missing in any cognitive domain). Missing data were imputed using the Missing Data Imputation (MDI) Toolbox for MATLAB 20,21. Briefly, missing data were firstly replaced by the mean of their corresponding test scores and partial least squares (PLS) was used to build the statistical model with a response matrix. The original test score matrix and the response matrix were auto-scaled to fit a PLS model to predict the missing values. Autoscaling and model fitting was iterated until convergence was reached.

Image acquisition

Participants were scanned on a 3 Tesla Siemens Tim Trio scanner using a 12-channel head coil (Erlangen, Germany). The scan protocol comprised a high-resolution magnetization prepared rapid gradient recalled echo (MPRAGE) sequence (repetition time (TR) = 1900 ms, echo time (TE) = 2.55 ms, inversion time = 900 ms, flip angle = 9°, 160 sagittal slices, matrix size = 256 × 256, voxel size = 1 mm isotropic) and a 3D SPACE-fluid attenuated inversion recovery (FLAIR) sequence (TR = 6000 ms, TE = 380 ms, inversion time = 2100 ms, flip angle = 120°, 160 axial slices, matrix size = 256 × 256, voxel size = 1mm isotropic).

Image processing

Infarcts were manually traced on the fluid-attenuated inversion recovery (FLAIR) image and verified by a stroke neurologist (A. B.). Infarcts were converted into a binary lesion map (see Supplementary Materials Section 3, Figure S1 for the group lesion overlap map). The individual FLAIR image, T_1-weighted image, and binarised lesion maps were used as inputs to perform lesion filling to correct the intensity of the lesions using the Lesion Segmentation Tool (LST) 22 for Statistical Parametric Mapping (SPM12; Wellcome Trust Centre for Neuroimaging). The LST creates a lesion probability map from the grey matter (GM), white matter (WM), and cerebrospinal fluid (CSF) segmented T1-weighted image. The intensity distribution is calculated using the FLAIR image based on these three tissue classes. The resultant lesion probability map combined with a binarized lesion map were used to fill lesions based on local information, to increase the accuracy of lesion filling. After lesion filling, we then applied the longitudinal VBM pipeline using a computational anatomy toolbox (CAT12) for SPM12 on the lesion-filled T_1-weighted images. Subject-level GM probability maps were obtained from T_1-weighted images following our previous approach [23], including (i) inter- participant image realignment across timepoints and intra-participant signal inhomogeneity correction for each participant to create a mean reference image for each subject; (ii) segmentation of the bias-corrected and reference images into GM, WM, and CSF using an Adaptive Maximum A Posterior (AMAP) technique 24; (iii) an initial affine registration applied to the bias-corrected image to improve the initial SPM segmentation; (iv) nonlinear Diffeomorphic Anatomical Registration Through Exponentiated Lie Algebra (DARTEL) registration 25 from all subjects to create a study-specific template in MNI space; (v) spatial normalisation of each segmented GM/WM reference image and individual GM/WM probability maps to the customised template in MNI space; (vi) modulation by multiplying voxel values with the linear and nonlinear component of the Jacobian determinant; (vii) smoothing on the normalized GM and WM probability maps with an isotropic 8 mm Gaussian kernel. An overview of the preprocessing and structural covariance pipeline is illustrated in Figure 1.

Structural covariance network (SCN) analysis

Region of interest (ROI) derivation

Six canonical brain networks were selected corresponding to cognitive domains tested in this study, including the dorsal attention (DAN), executive control (ECN), salience (SN), default mode (DMN), language-related (LN), and memory (MN) networks. For each network, two ROIs were chosen from the peak foci reported in previous studies (Table S2, Figure 1). We selected seed regions for each network on the basis that they have been shown to reliably produce the relevant network across a range of methods and imaging modalities. In particular, we selected networks that have been shown to be related to the associated cognitive domain tested here, and have been shown to be mirrored within structural covariance networks. The seed for the dorsal attention network represents the peak region derived from a meta-analysis of attention-related tasks 26. We chose this region because it is reliably activated in response to the top-down directed, voluntary deployment of attention as required by the behavioural attention tasks in our cognitive battery 26,27. Furthermore, the network shows correlated spontaneous activity even in the absence of a task 27,28. The seeds for the salience and executive control networks were derived from Seely et al., 2007 29. The seeds represent the peak regions of activation from executive control tasks and tasks requiring personal salience or interoceptive processing 29. The resultant dissociable networks can be reliably derived from task-based functional MRI, seed-based and independent component analysis of resting-state MRI 29. Importantly, these networks are also mirrored in structural covariance networks which show syndrome specific atrophy across dementia subtypes 15,17. Language network seeds were selected in a similar way, from the peak regions in a language network derived in healthy controls that was mirrored as a structural covariance network and that showed atrophy in language impaired dementia syndromes 15,30. For the default mode network, seeds that have been used previously in the derivation of task-based 31, resting-state 32,33 and structural covariance networks 16 were used. Finally, ROIs for the memory network were derived from peak regions in memory task-based fMRI 34 that also produces the hippocampal cortical network when used in seed-based resting state functional connectivity analysis 35.

We quantified the degree of overlap between the group lesion map and a conjunction map of all the ROI seeds (see Supplementary Materials Section 3, Figure S1) to ensure our results were not driven by damage within the seed regions. Four-mm radius spherical ROIs were used to extract the mean GM volume from the preprocessed GM probability maps using MarsBaR region of interest toolbox for SPM12. Notably, for the change of GM volume, we subtracted the GM probability maps at the subacute timepoint from the maps at the chronic timepoint for each subject and the resultant GM probability maps were used to extract mean change of GM volume with twelve 4-mm radius spherical ROIs.

Structural covariance network derivation

Seed partial least squares (PLS) was used to estimate structural covariance of each canonical brain network 36. Open source PLS software written in MATLAB (*https://www.rotman-baycrest.on.ca/index.php?section = 84)* 37 was used for all PLS analyses. The input to the seed PLS was the extracted mean GM volume of each seed and the preprocessed, whole-brain GM images (thresholded at signal intensity 0.45). To derive the covarying pattern between the seed GM volume and the rest of the

brain, we performed singular value decomposition (SVD) on the mean-centred and normalised input 38, a matrix in which rows correspond to participants and columns correspond to brain GM voxels. As such, structural covariance is estimated on a group level in order to show dominant covariation patterns in morphology across the brain.

The covariation pattern, formally known as latent variables (LVs), carries two key pieces of information. The first one is a voxel-wise 'brain salience' 3D volume that shows the structural covariation pattern. Voxels showing higher salience value have stronger associations with the seed GM; i.e., the core regions in the SCN. The second one is a set of summary scores, called 'brain scores', which can be used to make individual level inferences. Briefly, a brain score for each participant was derived by multiplying the whole-brain GM images and the right singular matrix (i.e., brain salience), serving as an estimate of individual-level covariance. Thus, participants whose GM morphology showed higher resemblance to the group-level structural covariance had higher brain scores. The statistical significance of an LV was evaluated using a permutation test (i.e. if the covariance accounted for by the seed GM exceeded what could be obtained by chance, estimated by randomly permuting the input matrix rows 5000 times). The stability of each voxel in the brain salience of the LV was quantified using a bootstrap ratio, calculated by dividing the voxel salience value by its standard error (i.e., akin to a Z- score), estimated by bootstrapping (resampling of input matrix rows 1000 times). Voxels with high bootstrap ratios contribute most to the brain covariation pattern.

To control for potential influences of confounding variables, separate linear regression analyses were performed on the brain scores of each seed for the subacute timepoint and longitudinal change. For the subacute timepoint, the variable of interest was the brain score of the seed. The confounding variables were age, sex, handedness, log-transformed infarct volume, and total intracranial volume. For change, the scan interval was input as an additional confounding variable. The unstandardised residual brain scores of twelve seeds, referred to as the SCN scores, were used for further behavioural PLS analysis.

To ensure that the results were not driven by global atrophy, we also tested the discovery and validation models, replacing total intracranial volume with grey matter volume or total brain volume (grey and white matter volume) normalised by total intracranial volume (see Supplementary Materials Section 5). For the longitudinal analyses we additionally controlled for change in global atrophy (chronic-subacute global atrophy; see Supplementary Materials 5.2).

Statistical Analysis

Behavioural partial least squares (PLS) analysis

Similar to the seed PLS, behavioural PLS was performed to investigate the multivariate relationships between the neuropsychological test scores and the SCN scores. The neuropsychological test scores were unstandardised residuals following linear regression to control for confounding variables. The

dependent variable was the score of each neuropsychological test and the confounding variables were age, sex, handedness, log- transformed infarct volume, and total intracranial volume. Similarly, the scan interval was input as an additional confounding variable in the longitudinal analysis. The behavioural PLS model examined the 17 neuropsychological test scores and 12 network-specific SCN scores at the subacute timepoint. The behavioural score was also derived by multiplying neuropsychological test scores and behavioural salience to estimate the test-dependent differences in the SCN-cognition correlation. Identical to the SCN only analysis, statistical significance and the importance and reliability of each test score in the SCN-cognition relationship were evaluated with permutation tests based on 5000 repetitions and bootstrapping based on 1000 repetitions, respectively.

A second behavioural PLS model was built to study the relationship between changes in neuropsychological test scores and changes in SCNs from subacute (3-months) to chronic (1-year) stroke following the procedure outlined in the first behavioural PLS model. Changes in 17 neuropsychological test scores and 12 network-specific SCN change scores were input into this second behavioural PLS model with the same permutation and bootstrapping procedures.

Two additional infarct volume control analyses for the subacute timepoint and change from subacute to chronic timepoint were performed without controlling for the infarct volume (Supplementary Materials Section 4).

The independent validation dataset was processed in exactly the same way, without any exceptions, at the subacute timepoint (Supplementary Materials Section 5). Due to a low sample size at the chronic timepoint, we used split half validation, repeated five times with random sampling (Supplementary Materials Section 6.2).

Data availability

The data that support the findings of this study are available from the corresponding author upon reasonable request.

Results

Relationship between structural covariance networks and cognitive function in subacute stroke

We derived canonical SCNs using twelve seeds from six major brain networks underlying cognitive function at the subacute timepoint (Figure 2, surface rendered in Supplementary Materials Section 7, Figure S9). A latent variable (LV1) significantly contributed to twelve SCNs (p = 0.001) and explained 99.83% of the variance in the behavioural PLS model. There was a positive correlation between the behavioural and brain scores (r = 0.194, p < 0.001, Figure 3A). All SCNs contributed fairly equally and significantly to LV1 with less than −2 bootstrap ratio (akin to Z-score) 37 (Figure 3B). The corresponding

neuropsychological tests revealing the strongest correlations of LV1 were the Digit Span Task (r = −0.222, 95% confidence interval [C. I.] −0.379——0.059), Trail-Making test (A) (TMT-A) (r = −0.311, 95% C. I. −0.437——0.181) and Simple Reaction Time task (r = −0.213, 95% C. I. −0.374——0.047) in the attention domain, the Trail-Making test (B) (TMT-B) (r = −0.175, 95% C. I. −0.333 – −0.039) in the executive function domain, the Boston Naming Test (BNT) (r = −0.254, 95% C. I. −0.411 – −0.037) and Controlled Oral Word Association Test (COWAT)-animals (r = −0.178, 95% C. I. −0.337——0.037) in the language domain, the Hopkins Verbal Learning Test (HVLT)-Delay (r = −0.146, 95% C. I. −0.280 – −0.012) in the memory domain and the Rey Complex Figure (RCF)- copy (r = −0.165, 95% C. I. −0.334——0.009) in the visuospatial function domain (Figure 3C). These results suggested that more damaged SCNs were related to worse attention, executive function, language, memory and visuospatial function performance at the subacute timepoint. An additional control analysis without correcting for infarct volume revealed highly similar results, indicating that our findings were robust (Supplementary Materials Section 4, Figure S2). Further analyses controlling for global brain atrophy also replicated these findings (see Supplementary Section 5.1, Figure S4). Finally, we tested the model in an independent validation. Replicating the main results, a single LV explained 87.18% of the variance in the behavioural PLS model (p < 0.001) and all twelve SCNs significantly contributed to this LV (Supplementary Materials Section 6.1, Figure S6). The significant correlation between brain and behavioural scores was also replicated (r = 0.325, p < 0.001). Additional analyses controlling for GM/TIV or GM+WM/TIV again demonstrated similar findings (Supplementary Materials Section 6.1, Figure S7).

Relationship between changes in structural covariance networks and changes in cognitive function

We derived networks based on the covariance of the rate of change in grey matter volume from subacute to chronic stroke. Importantly, the regions showing significant covariation with the seeds mirror those shown in the SCNs derived at the subacute timepoint (Figure 2, surface rendered Figure S9). This confirms covariation in the change in grey matter volume occurs within the domain specific canonical networks, albeit to a reduced spatial extent. After applying behavioural PLS, one significant LV was identified for SCNs (p < 0.001) and it explained 64.91% of variance of the PLS model. A positive correlation between the behavioural and brain scores (r = 0.287, p < 0.001) was once again noted (Figure 4A). All SCNs except right hippocampus (HIPP) and right dorsolateral prefrontal cortex (DLPFC) showed stable negative weightings (Figure 4B). The corresponding neuropsychological tests showing significant correlations were the choice reaction time task (r = 0.256, 95% C. I. 0.449 – 0.078) in the attention domain, the controlled word association test-FAS in the language domain (r = 0.188, 95% C. I. 0.357 – 0.010), and RCF-delay (r = 0.316, 95% C. I. 0.468 – 0.139) in the memory domain (Figure 4C). Highly similar results were found in a control analysis without correcting for infarct volume (Supplementary Materials Section 4, Figure S3). In the split half validation, we found a single latent variable (p < 0.001) accounting for between 41.15 and 60.10 % of the variance in the PLS model across 10 split half samples (Supplementary Materials Section 6.2, Table S4). The first iteration of split half validation analysis

showed a correlation between behavioural change and change in SCN brain scores of similar magnitude to the discovery analysis (r = 0.435, sample 1 and r = 0.465, sample 2 (p < 0.001), Supplementary Materials Section 6.2, Figure S8).

Discussion

Cognitive decline is common after ischaemic stroke 1,2 but has proved difficult to predict because the effects of stroke are not limited to the primary neuroanatomical location of brain damage. Functional networks based on correlated brain activity, and structural networks based on white matter fibre connections have been extensively studied in stroke 5,6,39 and reflect widespread disruption, despite focal and heterogenous damage caused by stroke. In contrast, there has been much less investigation of SCNs in stroke, despite their potential to clarify patterns of distributed atrophy, or reflect recovery-related plasticity 13,40. We used a novel, data driven method, taking advantage of our unique longitudinal data to examine covariance in the rate of change in SCNs from subacute to chronic stroke. Crucially, we sought to determine if these SCNs and their longitudinal change had cognitive consequences by examining the relationship to cognitive performance and cognitive decline across domains. We show cognitive decline after ischaemic stroke is associated with degeneration of canonical SCNs.

Structural covariance of the default mode, dorsal attention, executive control, salience, memory and language-related networks was associated with cognitive performance in the attention, executive function, language, memory and visuospatial domains, showing an association between topographical network organisation in subacute stroke and cognitive performance. SCNs seeded from known network nodes replicated the topographical pattern of known functionally specific networks. Using a global ‘brain score’ and ‘behavioural score’ estimated from the PLS model, we found a significant correlation showing cognitive impairment associated with more damaged SCNs that we replicated in the independent validation dataset. Structural covariance of major canonical networks is associated with cognitive performance in subacute stroke. Specifically, more damaged SCNs were related to deficits in attention, executive function, language, memory and visuospatial function. Attention was most implicated in this analysis with three tests of attention covarying with the SCN latent variable, compared to a single test in other domains. This may reflect the frequency of attentional impairment seen in subacute stroke, or the overlap of attentional functions across other cognitive domains.

As a further test of whether SCN integrity was associated with cognitive impairment after stroke, we examined covariance in the rate of longitudinal change in major brain networks and related this to changes in cognitive performance between subacute and chronic stroke. Covariance networks mirrored the SCNs derived at the subacute timepoint, suggesting grey matter volume changes from the subacute to chronic phase were occurring within established, domain-specific networks. The greatest changes, in terms of extent of distributed spatial covarying patterns, were in the default mode network and dorsal attention network.

Degeneration of the major SCNs was associated with cognitive decline, specifically in the attention, memory and language domain. These results suggested that faster degradation of SCNs of bilateral dorsal attention, default mode, language-related networks as well as left dorsolateral prefrontal cortex, hippocampus and frontal insula were related to greater decline in attention, language and memory performance. These two findings are important, but should not be surprising, given that attentional deficits are a consistent feature of post-stroke cognitive impairment. Indeed, the most frequently impaired domains after ischaemic stroke are attention, memory and language 41. Up to 70% of patients have impaired speed of processing and attention after stroke. 1,42,43. Similarly, memory problems are a frequent complaint after stroke, with estimates around 23–55% of patients are affected at three months post-stroke and 11–31% affected at one year 44,45. Our work suggests at least some of this attention, memory and language impairment may be driven by widespread degeneration of SCNs from the subacute to chronic phase. Developmental SCN changes 30, as well as in normal aging and neurological diseases 12,13, have been well characterised. They have rarely associated with cognitive measures, and not been well investigated after ischaemic stroke.

What might be the mechanism resulting in widespread SCN changes, across all networks, after ischaemic stroke, even after accounting for age-related degeneration? Stroke may initiate or aggravate neurodegenerative processes above that seen in healthy aging 46. One plausible mechanism for widespread structural changes as the result of focal ischaemic stroke is secondary Wallerian degeneration due to disconnection between brain regions as a result of the stroke 47. If a brain region, or multiple brain regions in the case of complex networks, are disconnected after stroke, there may be degeneration as a result of underutilisation of the disconnected region that results in volume loss 47. Alternatively, stroke may initiate an ischaemic cascade that results in neurodegenerative processes leading to widespread brain atrophy 46,48,49. Given the timescale of the atrophic changes (3-months and 1-year post-stroke) and how widespread they are in nature, a more plausible alternative is that stroke occurred on a background of accelerated atrophy as the result of cerebrovascular burden 9,50. Future work should examine the clinical characteristics that predict widespread SCN degeneration associated with cognitive impairment.

The work should be interpreted in light of its limitations. As is often the case, the heterogeneity observed within stroke cohorts precludes detailed examination of different profiles of cognitive impairments as the sample size of each subgroup was too small for adequate statistical power. We controlled for infarct volume in the analysis, but did not take into account location, again the heterogeneity of the stroke types and infarct locations, make sub-group analyses under-powered. We conducted an independent validation analysis and confirmed our main findings, namely one significant latent variable accounting for most of the variance in the seed PLS models. Fairly equal contributions from all SCNs as well as significant correlations between brain and behavioural scores were observed in the subacute model, which is similar to the findings in the discovery analysis. However, there were some differences related to the SCN profiles and neuropsychological tests that correlated with the latent variable in the longitudinal model. This may be the result of the sample size used in the validation sample (one third of the discovery sample). Alternatively, this might reflect a degree of dynamic change in cognition at this timepoint. Cognition is

likely to stabilise as the time from the stroke increases. Future work will examine the longitudinal effects at even longer, likely even more stable time points collected in this protocol (up to five years). As a group, the median stroke severity (as measured by mRS and NIHSS) was relatively mild. Although this may limit generalisability of the finding to cohorts with more severe stroke, it also raises the possibility that SCNs and cognition maybe even more disrupted when stroke is not as mild as in this cohort. Finally, we carefully chose the seeds to derive our structural covariance networks based on the existing literature. Emerging large functional network atlases 51–53 could be employed to facilitate seed definitions to produce structural covariance networks 54. Future work should aim to replicate our findings to ensure it is robust to seed location.

Summary

Cognitive decline after ischaemic stroke has been difficult to predict due to widespread effects of stroke on the brain. Using data-driven multivariate methods to examine cognition and canonical brain networks across cognitive domains, we show that structural covariance integrity of cognitive networks is associated with cognition at three months post-stroke and with longitudinal cognitive decline in attention, memory and language from subacute to chronic stroke. Structural covariance analyses of brain networks reveal widespread network disruptions associated with cognitive decline.

Declarations

Acknowledgements

We thank our participants and their caregivers who generously volunteered their time to take part in the study.

Sources of funding

This research was supported by the National Medical Research Council, Singapore (NMRC/CIRG/1390/2014 and NMRC0088/2015), and the Duke-NUS Medical School Signature Research Program funded by Ministry of Health, Singapore (J. H. Z.) and National Health and Medical Research Council project grant (GNT1020526), the Brain Foundation, Wicking Trust, Collie Trust, and Sidney and Fiona Myer Family Foundation (A. B.) as well as The Royal Society Commonwealth Science Conference Follow-On Grant (M. V.).

Competing interests

There are no competing interests to declare.

Author contributions

M. V., J. H. Z., and A. B. contributed to the study design, results interpretations, and manuscript preparation; H.-J. C. and M. V. performed the data analysis, interpretations, and manuscript preparation; E. W., M. S. K., and A. B. contributed to data collection; F. J., K. K. N., J. K. W. L., X. Q., and H. Y. assisted in data analysis and discussion.

References

1. Hochstenbach, J., Mulder, T., van Limbeek, J., Donders, R. & Schoonderwaldt, H. Cognitive decline following stroke: A comprehensive study of cognitive decline following stroke. *Journal of Clinical and Experimental Neuropsychology* **20**, 503-517, doi:10.1076/jcen.20.4.503.1471 (1998).
2. Levine, D. A. *et al.* Trajectory of cognitive decline after incident stroke. *JAMA* **314**, 41-51, doi:10.1001/jama.2015.6968 (2015).
3. Cumming, T. B., Brodtmann, A., Darby, D. & Bernhardt, J. The importance of cognition to quality of life after stroke. *Journal of Psychosomatic Research* **77**, 374- 379, doi:10.1016/j.jpsychores.2014.08.009 (2014).
4. Fox, M. D. Mapping symptoms to brain networks with the human connectome. *The New England Journal of Medicine* **379**, 2237-2245, doi:10.1056/NEJMra1706158 (2018).
5. Grefkes, C. & Fink, G. R. Connectivity-based approaches in stroke and recovery of function. *The Lancet Neurology* **13**, 206-216, doi:10.1016/S1474-4422(13)70264-3 (2014).
6. Grefkes, C. & Fink, G. R. Reorganization of cerebral networks after stroke: new insights from neuroimaging with connectivity approaches. *Brain* **134**, 1264-1276, doi:10.1093/brain/awr033 (2011).
7. Siegel, J. S. *et al.* Disruptions of network connectivity predict impairment in multiple behavioral domains after stroke. *Proceedings of the National Academy of Sciences of the United States of America* **113**, E4367-E4376, doi:10.1073/pnas.1521083113 (2016).
8. Stinear, C. M. *et al.* Functional potential in chronic stroke patients depends on corticospinal tract integrity. *Brain* **130**, 170-180, doi:10.1093/brain/awl333 (2007).
9. Werden, *et al.* Structural MRI markers of brain aging early after ischemic stroke. *Neurology* **89**, 116-124, doi:10.1212/WNL.0000000000004086 (2017).
10. Veldsman, M., Curwood, E., Pathak, S., Werden, E. & Brodtmann, A. Default mode network neurodegeneration reveals the remote effects of ischaemic stroke. *Journal of Neurology, Neurosurgery & Psychiatry* **89**, 318-320, doi:10.1136/jnnp-2017-315676 (2018).
11. Firbank, M. J. *et al.* Medial temporal atrophy rather than white matter hyperintensities predict cognitive decline in stroke survivors. *Neurobiology of Aging* **28**, 1664-1669, doi:10.1016/j.neurobiolaging.2006.07.009 (2006).

12. Evans, A. C. Networks of anatomical covariance. *NeuroImage* **80**, 489-504, doi:10.1016/j.neuroimage.2013.05.054 (2013).
13. Spreng, R. N. & Turner, G. R. Structural covariance of the default network in healthy and pathological aging. *The Journal of Neuroscience* **33**, 15226-15234, doi:10.1523/JNEUROSCI.2261-13.2013 (2013).
14. Veldsman, M. Brain atrophy estimated from structural magnetic resonance imaging as a marker of large-scale network-based neurodegeneration in aging and stroke. *Geriatrics* **2**, doi:10.3390/geriatrics2040034 (2017).
15. Seeley, W. W., Crawford, R. K., Zhou, J., Miller, B. L. & Greicius, M. D. Neurodegenerative diseases target large-scale human brain networks. *Neuron* **62**, 42- 52, doi:10.1016/j.neuron.2009.03.024 (2009).
16. Zhou, J., Gennatas, Efstathios D., Kramer, Joel H., Miller, Bruce L. & Seeley, William W. Predicting regional neurodegeneration from the healthy brain functional connectome. *Neuron* **73**, 1216-1227, doi:10.1016/j.neuron.2012.03.004 (2012).
17. Zhou, J. *et al.* Divergent network connectivity changes in behavioural variant frontotemporal dementia and Alzheimer's disease. *Brain* **133**, 1352 (2010).
18. Zhou, J. & Seeley, W. W. Network dysfunction in Alzheimer's disease and frontotemporal dementia: implications for psychiatry. *Biological Psychiatry* **75**, 565, doi:10.1016/j.biopsych.2014.01.020 (2014).
19. Brodtmann, A. *et al.* Charting cognitive and volumetric trajectories after stroke: Protocol for the cognition and neocortical volume after stroke (CANVAS) study. *International Journal of Stroke* **9**, 824-828, doi:10.1111/ijs.12301 (2014).
20. Folch-Fortuny, A., Arteaga, F. & Ferrer, A. Missing data imputation toolbox for MATLAB. *Chemometrics and Intelligent Laboratory Systems* **154**, 93-100, doi:https://doi.org/10.1016/j.chemolab.2016.03.019 (2016).
21. Folch-Fortuny, A., Arteaga, F. & Ferrer, A. PLS model building with missing data: New algorithms and a comparative study. *Journal of Chemometrics* **31**, e2897, doi:10.1002/cem.2897 (2017).
22. Schmidt, *et al.* An automated tool for detection of FLAIR-hyperintense white-matter lesions in Multiple Sclerosis. *Neuroimage* **59**, 3774-3783, doi:10.1016/j.neuroimage.2011.11.032 (2012).
23. Ng, K. K., Lo, J. C., Lim, J. K. W., Chee, M. W. L. & Zhou, J. Reduced functional segregation between the default mode network and the executive control network in healthy older adults: A longitudinal study. *NeuroImage* **133**, 321-330, doi:https://doi.org/10.1016/j.neuroimage.2016.03.029 (2016).
24. Rajapakse, C., Giedd, J. N. & Rapoport, J. L. Statistical approach to segmentation of single-channel cerebral MR images. *IEEE Transactions on Medical Imaging* **16**, 176- 186, doi:10.1109/42.563663 (1997).
25. Ashburner, J. A fast diffeomorphic image registration algorithm. *NeuroImage* **38**, 95- 113, doi:10.1016/j.neuroimage.2007.07.007 (2007).

26. Corbetta, M. & Shulman, G. L. Control of goal-directed and stimulus-driven attention in the brain. *Nature Reviews Neuroscience* **3**, 201-215, doi:10.1038/nrn755 (2002).
27. Fox, M. D., Corbetta, M., Snyder, A. Z., Vincent, J. L. & Raichle, M. E. Spontaneous neuronal activity distinguishes human dorsal and ventral attention systems. *Proceedings of the National Academy of Sciences* **103**, 10046, doi:10.1073/pnas.0604187103 (2006).
28. Vossel, , Geng, J. J. & Fink, G. R. Dorsal and ventral attention systems: distinct neural circuits but collaborative roles. *Neuroscientist* **20**, 150-159, doi:10.1177/1073858413494269 (2014).
29. Seeley, W. *et al.* Dissociable intrinsic connectivity networks for salience processing and executive control. *The Journal of Neuroscience* **27**, 2349, doi:10.1523/JNEUROSCI.5587-06.2007 (2007).
30. Zielinski, B. A., Gennatas, E. D., Zhou, J. & Seeley, W. W. Network-level structural covariance in the developing brain. *Proceedings of the National Academy of Sciences* **107**, 18191, doi:10.1073/pnas.1003109107 (2010).
31. Sridharan, D., Levitin, D. J. & Menon, V. A critical role for the right fronto-insular cortex in switching between central-executive and default-mode *Proceedings of the National Academy of Sciences* **105**, 12569, doi:10.1073/pnas.0800005105 (2008).
32. Chong, J. S. X. *et al.* Influence of cerebrovascular disease on brain networks in prodromal and clinical Alzheimer's disease. *Brain* **140**, 3012-3022, doi:10.1093/brain/awx224 (2017).
33. Greicius, D., Krasnow, B., Reiss, A. L. & Menon, V. Functional connectivity in the resting brain: A network analysis of the default mode hypothesis. *Proceedings of the National Academy of Sciences* **100**, 253, doi:10.1073/pnas.0135058100 (2003).
34. Koechlin, E., Basso, G., Pietrini, P., Panzer, S. & Grafman, J. The role of the anterior prefrontal cortex in human *Nature* **399**, 148-151, doi:10.1038/20178 (1999).
35. Vincent, L., Kahn, I., Snyder, A. Z., Raichle, M. E. & Buckner, R. L. Evidence for a frontoparietal control system revealed by intrinsic functional connectivity. *J Neurophysiol* **100**, 3328-3342, doi:10.1152/jn.90355.2008 (2008).
36. McIntosh, A. R. & Lobaugh, N. J. Partial least squares analysis of neuroimaging data: applications and *NeuroImage* **23**, S250-S263, doi:https://doi.org/10.1016/j.neuroimage.2004.07.020 (2004).
37. Krishnan, A., Williams, L. J., McIntosh, A. R. & Abdi, H. Partial Least Squares (PLS) methods for neuroimaging: A tutorial and review. *NeuroImage* **56**, 455-475, doi:10.1016/j.neuroimage.2010.07.034 (2011).
38. Eckart, & Young, G. The approximation of one matrix by another of lower rank. *Psychometrika* **1**, 211-218, doi:10.1007/BF02288367 (1936).
39. Bullmore, E. & Sporns, O. Complex brain networks: graph theoretical analysis of structural and functional systems. *Nature Reviews Neuroscience* **10**, 186-198, doi:10.1038/nrn2575 (2009).
40. Abela, E. *et al.* A thalamic-fronto-parietal structural covariance network emerging in the course of recovery from hand paresis after ischemic stroke. *Frontiers in neurology* **6**, 211, doi:10.3389/fneur.2015.00211 (2015).

41. Gottesman, R. F. M. D. & Hillis, A. E. P. Predictors and assessment of cognitive dysfunction resulting from ischaemic stroke. *Lancet Neurology* **9**, 895-905, doi:10.1016/S1474-4422(10)70164-2 (2010).
42. Barker-Collo, L. *et al.* Reducing attention deficits after stroke using attention process training: a randomized controlled trial. *Stroke* **40**, 3293-3298, doi:10.1161/STROKEAHA.109.558239 (2009).
43. Hyndman, D., Pickering, R. M. & Ashburn, A. The influence of attention deficits on functional recovery post stroke during the first 12 months after discharge from *Journal of Neurology, Neurosurgery & Psychiatry* **79**, 656-663, doi:10.1136/jnnp.2007.125609 (2008).
44. das Nair, , Cogger, H., Worthington, E. & Lincoln, N. B. Cognitive rehabilitation for memory deficits after stroke. *The Cochrane database of systematic reviews* **9**, CD002293, doi:10.1002/14651858.CD002293.pub3 (2016).
45. Snaphaan, L. J. A. E. & Leeuw, F. E. d. Poststroke memory function in nondemented patients: a systematic review on frequency and neuroimaging correlates. *Stroke* **38**, 198-203, doi:10.1161/01.STR.0000251842.34322.8f (2007).
46. Cumming, T. B. & Brodtmann, A. Can stroke cause neurodegenerative dementia? *International Journal of Stroke* **6**, 416-424, doi:10.1111/j.1747-4949.2011.00666.x (2011).
47. Duering, M. *et al.* Incident subcortical infarcts induce focal thinning in connected cortical regions. *Neurology* **79**, 2025-2028, doi:10.1212/WNL.0b013e3182749f39 (2012).
48. Xing, C., Arai, K., Lo, E. H. & Hommel, M. Pathophysiologic cascades in ischemic stroke. *International Journal of Stroke* **7**, 378-385, doi:10.1111/j.1747- 4949.2012.00839.x (2012).
49. Shi, K. *et al.* Global brain inflammation in stroke. *The Lancet Neurology* **18**, 1058- 1066, doi:10.1016/S1474-4422(19)30078-X (2019).
50. Knopman, D. S. & Hooshmand, B. Cerebrovascular disease affects brain structural integrity long before clinically overt strokes. *Neurology* **89**, 110-111, doi:10.1212/WNL.0000000000004098 (2017).
51. Yeo, T. T. *et al.* The organization of the human cerebral cortex estimated by intrinsic functional connectivity. *J Neurophysiol* **106**, 1125-1165, doi:10.1152/jn.00338.2011 (2011).
52. Power, Jonathan *et al.* Functional Network Organization of the Human Brain. *Neuron* **72**, 665-678, doi:https://doi.org/10.1016/j.neuron.2011.09.006 (2011).
53. Dosenbach, U. F. *et al.* Prediction of Individual Brain Maturity Using fMRI. *Science* **329**, 1358, doi:10.1126/science.1194144 (2010).
54. DuPre, E. & Spreng, R. N. Structural covariance networks across the life span, from 6 to 94 years of age. *Network Neuroscience* **1**, 302-323, doi:10.1162/NETN_a_00016 (2017).

Tables

Due to technical limitations, Table 1 is provided in the Supplementary Files section.

Figures

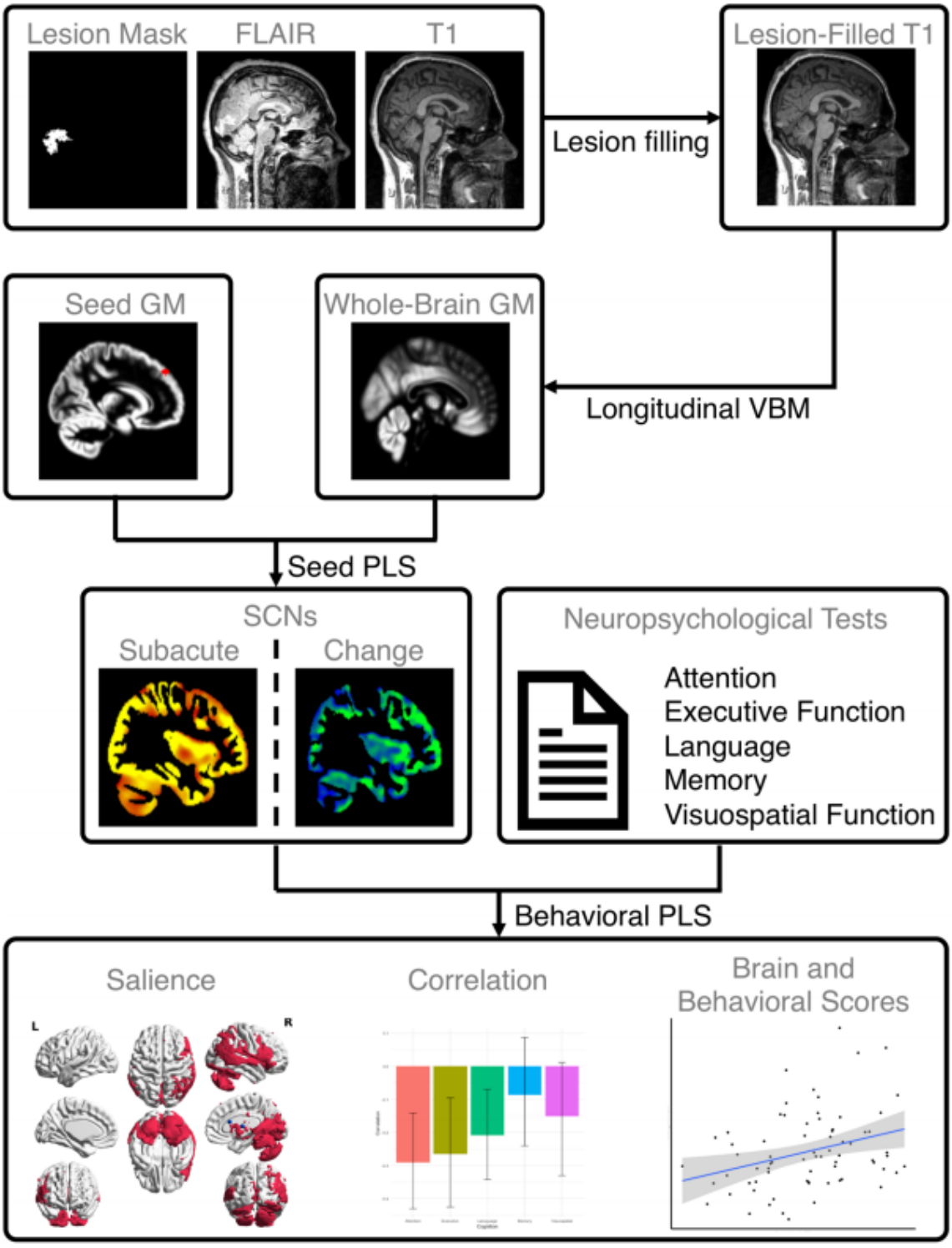

Figure 1

Overview of study design schematic. For each participant, we first used a lesion segmentation tool 22 with a lesion mask as well as FLAIR and T1-weighted images to generate a lesion-filled T1-weighted image for each participant. Then, we applied the longitudinal VBM pipeline using a computational anatomy toolbox (CAT12) to obtain smoothed and normalized GM images. With predefined regions of interest based on canonical brain networks, we extracted the mean GM volume of each seed. Seed PLS

was used to covary the seed and whole-brain GM for deriving the SCNs at three months post-stroke (subacute timepoint) and change from three months to one year (chronic timepoint) post-stroke, respectively, for all participants. Finally, SCN scores and neuropsychological test scores at the subacute timepoint were input into a behavioural PLS model to examine the covariance between SCNs and cognition for all participants. The SCN change scores and changes of neuropsychological test scores were input into another behavioural PLS model to investigate the cognitive decline over time based on SCN degradation from three months to one year post-stroke for all participants. Abbreviations: FLAIR – fluid-attenuated inversion recovery; GM – grey matter; PLS – partial least squares; SCN – structural covariance network; VBM – voxel-based morphometry.

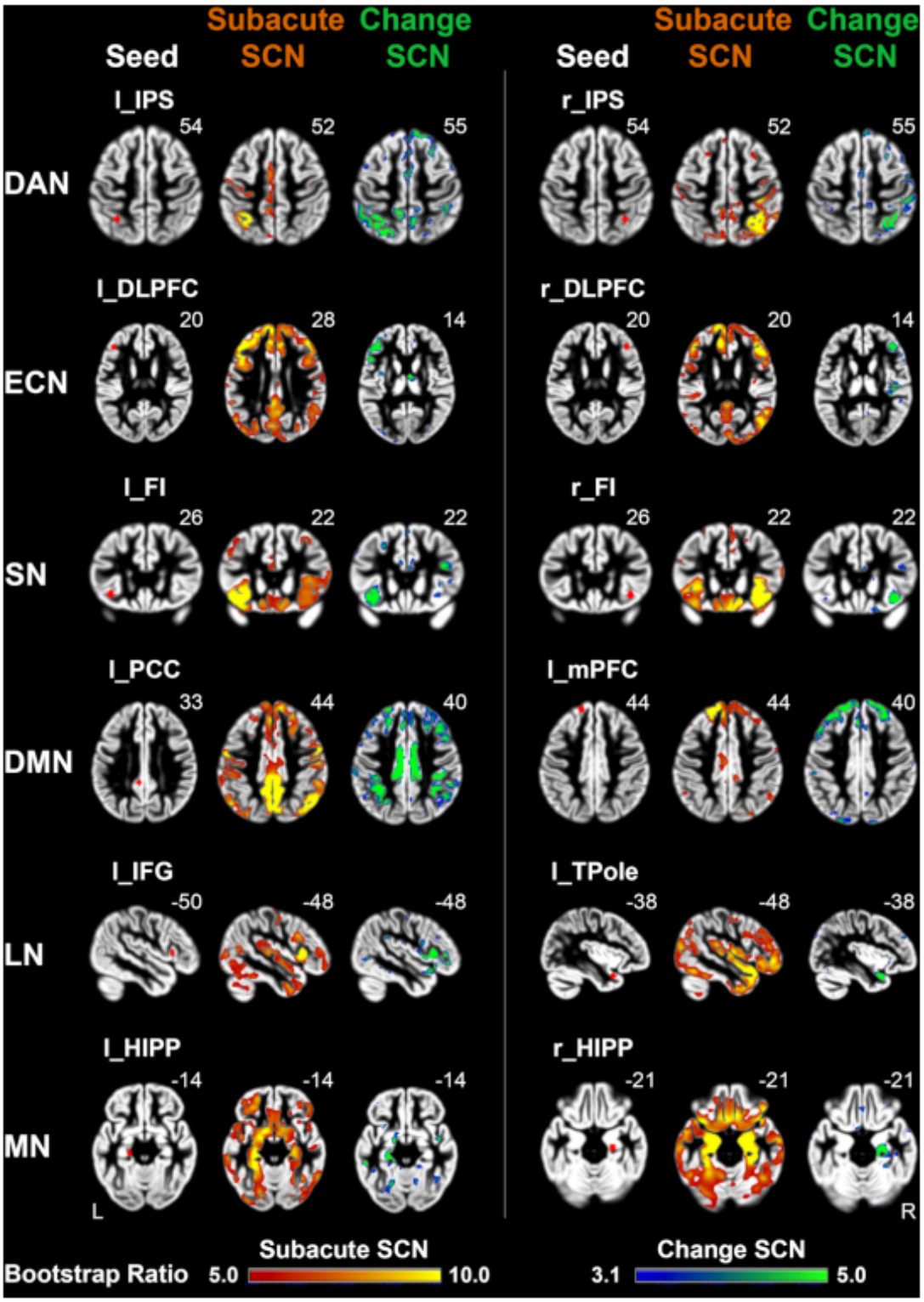

Figure 2

Seed regions of canonical brain networks and structural covariance networks in subacute and chronic stroke patients. For six canonical brain networks, two seed regions (red dot, first column) were selected for investigating the covarying patterns of structural covariance networks (SCNs). The derived structural covariance networks at the subacute timepoint (second column in orange) and for change from subacute to chronic stroke (third column in green). Abbreviations: DAN – dorsal attention network; DMN – default

mode network; ECN – executive control network; l_DLPFC – left dorsolateral prefrontal cortex; l_FI – left frontal insula; l_HIPP – left hippocampus; l_IFG – left inferior frontal gyrus; l_IPS – left intraparietal sulcus; l_mPFC – left medial prefrontal cortex; l_PCC – left posterior cingulate cortex; l_TPole – left temporal pole; LN – language-related network; MN – memory network; r_DLPFC – right dorsolateral prefrontal cortex; r_HIPP – right hippocampus; r_FI – right frontal insula; r_IPS – right intraparietal sulcus; SCN – structural covariance network; SN – salience network.

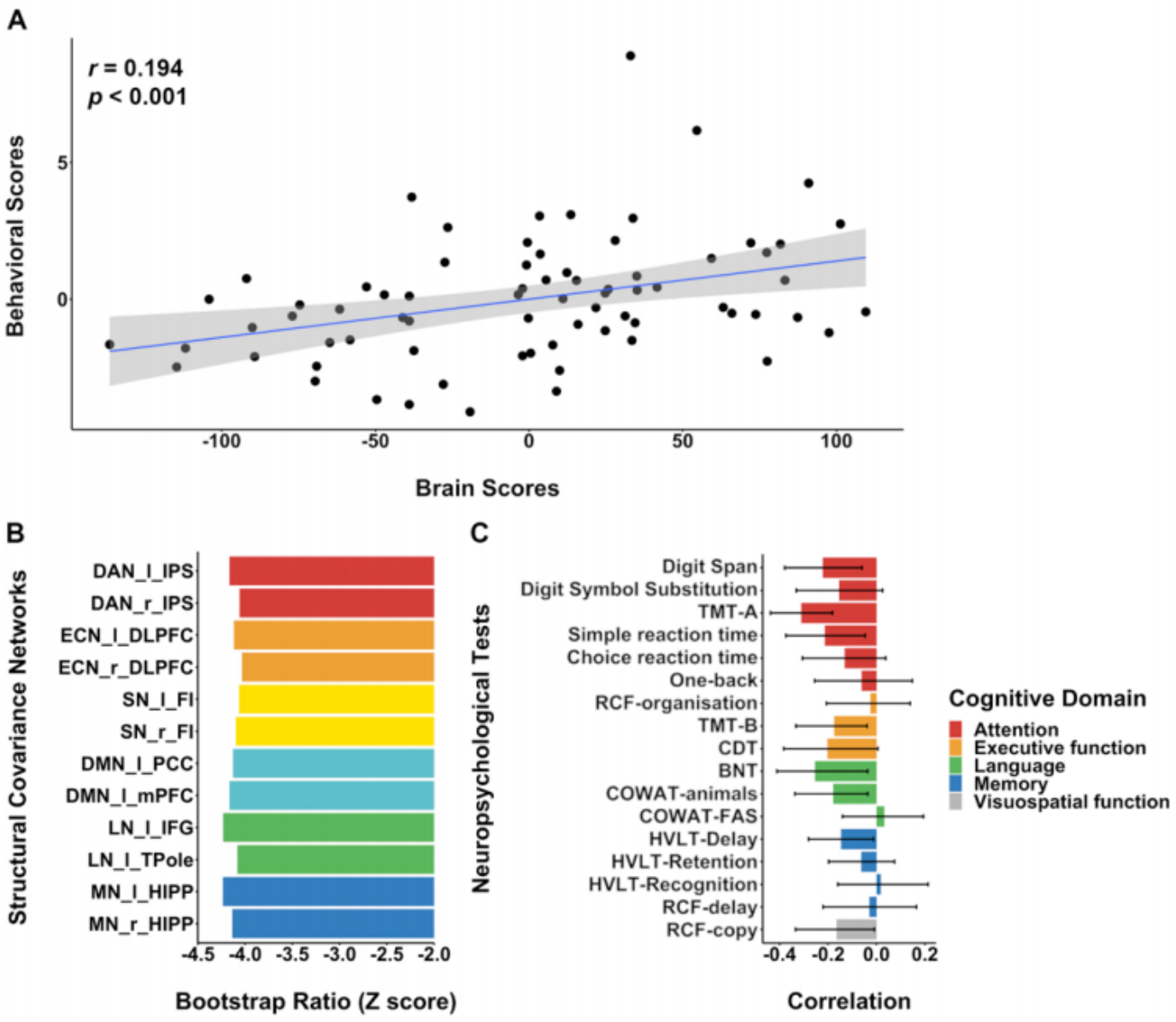

Figure 3

Lower baseline integrity of structural covariance networks was associated with greater impairment in cognitive performance in subacute stroke. (A) A positive correlation between behavioural and brain scores suggested more damaged SCNs were associated with worse attention, executive function, language, memory, and visuospatial function performance at 3-months post-stroke. (B) The bootstrap ratio (akin to a Z-score) demonstrated the contributions of each SCN to the covariance between SCNs

and neuropsychological tests. (C) Seventeen neuropsychological tests showed extensive negative correlations with SCNs, particularly in the Digit Span Task, TMT-A, and simple reaction time task within the attention domain, the TMT-B within the executive function domain, the BNT and COWAT-animals within the language domain, and the RCF-copy within the visuospatial domain. The error bars indicate 95% confidence interval. Abbreviations: BNT – Boston Naming Test; CDT – clock-drawing test; COWAT – Controlled Oral Word Association Test; DAN – dorsal attention network; DMN – default mode network; ECN – executive control network; HVLT – Hopkins Verbal Learning Test; l_DLPFC – left dorsolateral prefrontal cortex; l_FI – left frontal insula; l_HIPP – left hippocampus; l_IFG – left inferior frontal gyrus; l_IPS – left intraparietal sulcus; l_mPFC – left medial prefrontal cortex; l_PCC – left posterior cingulate cortex; l_TPole – left temporal pole; LN – language-related network; MN – memory network; r_DLPFC – right dorsolateral prefrontal cortex; r_HIPP – right hippocampus; r_FI – right frontal insula; r_IPS – right intraparietal sulcus; RCF – Rey Complex Figure; SCN – structural covariance network; SN – salience network; TMT-A – trail-making test (A); TMT-B – trail-making test (B).

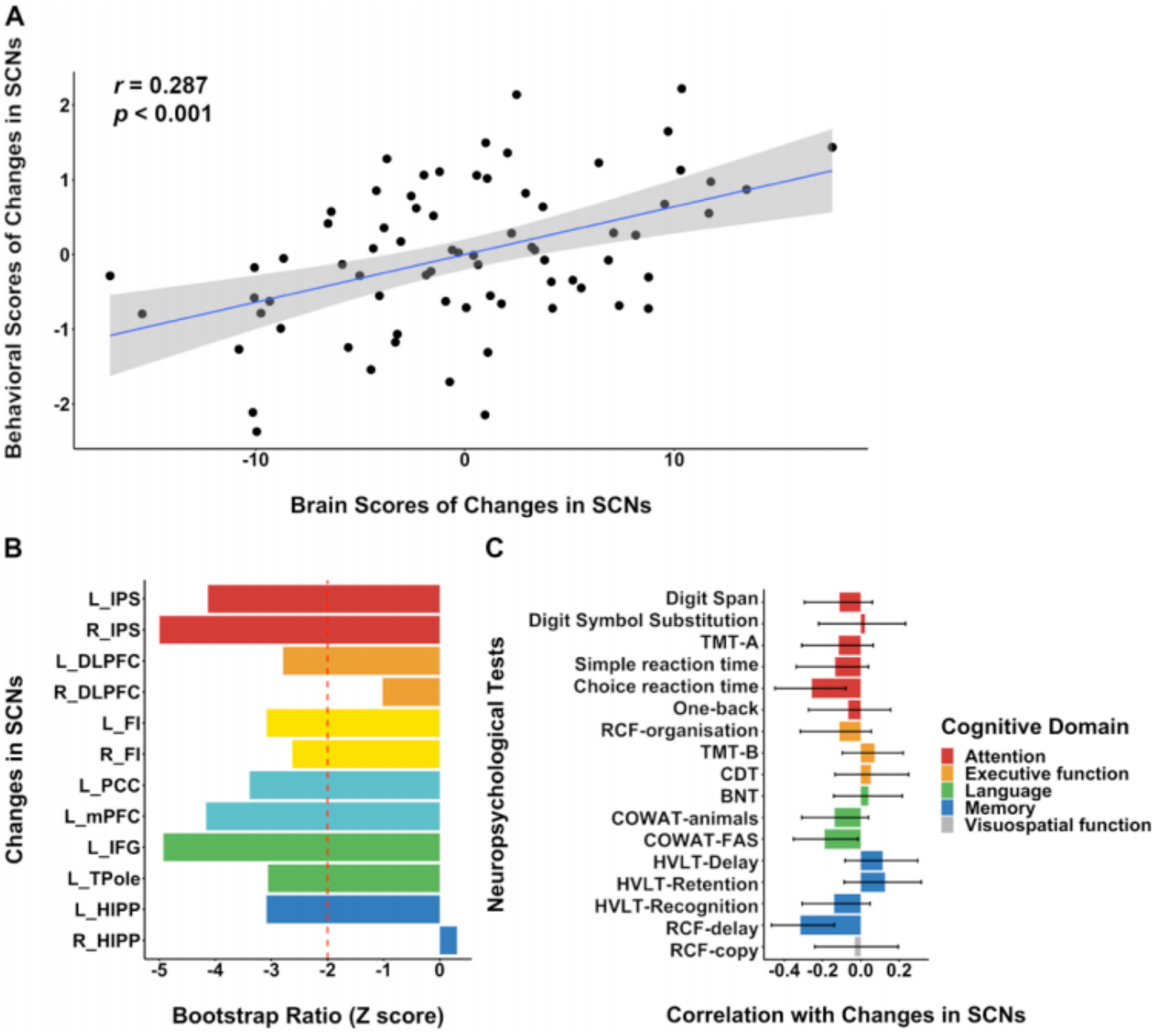

Figure 4

Faster degradation of structural covariance networks was associated with greater longitudinal decline in performance of attention, language and memory from three months to one-year post-stroke. (A) A positive correlation between changes in behavioural scores and changes in brain scores suggested faster SCN degeneration was associated with greater longitudinal decline in neuropsychological tests from three months to one-year post-stroke. (B) The bootstrap ratio demonstrated the contributions of each SCN to the covariance between SCNs and neuropsychological tests. (C) The significant correlation between each neuropsychological test and SCNs was shown in the choice reaction time task within the attention domain, the COWAT-FAS within the language domain, and the RCF-delay within the memory domain. The error bars indicate 95% confidence interval. Abbreviations: BNT – Boston Naming Test; CDT – clock-drawing test; COWAT – Controlled Oral Word Association Test; DAN – dorsal attention network; DMN –

default mode network; ECN – executive control network; HVLT – Hopkins Verbal Learning Test; l_DLPFC – left dorsolateral prefrontal cortex; l_FI – left frontal insula; l_HIPP – left hippocampus; l_IFG – left inferior frontal gyrus; l_IPS – left intraparietal sulcus; l_mPFC – left medial prefrontal cortex; l_PCC – left posterior cingulate cortex; l_TPole – left temporal pole; LN – language-related network; MN – memory network; r_DLPFC – right dorsolateral prefrontal cortex; r_HIPP – right hippocampus; r_FI – right frontal insula; r_IPS – right intraparietal sulcus; RCF – Rey Complex Figure; SCN – structural covariance network; SN – salience network; TMT-A – trail-making test (A); TMT-B – trail-making test (B).

Supplementary Files

This is a list of supplementary files associated with this preprint. Click to download.

- SupplMaterials.pdf
- Table1.docx